Meteorologische Zeitschrift, Vol. 23, No. 4, 441–447 (published online April 4, 2014)




# On the theory of mass conserving transformations for Lagrangian methods in 3D atmosphere-chemistry models

Volker Grewe[1*], Sabine Brinkop[1], Patrick Jöckel[1], Seoleun Shin[3], Sebastian Reich[2] and Harry Yserentant[4]

[1]Deutsches Zentrum für Luft- und Raumfahrt, Institut für Physik der Atmosphäre, Oberpfaffenhofen, Germany
[2]Institut für Mathematik, Universität Potsdam, Germany
[3]now at Korea Institute of Atmospheric Prediction Systems, Seoul, Korea
[4]Institut für Mathematik, Technische Unversität, Berlin, Germany

(Manuscript received November 22, 2013; in revised form February 4, 2013; accepted February 5, 2014)

**Abstract**

Lagrangian methods were used in the past for dispersion modelling, air quality studies and climate-chemistry simulations, because they have a good representation of tracer transport. Here we show that air density inconsistencies between the Lagrangian representation and the model's core grid can lead to substantial discrepancies. They affect any process calculation related to tracers on the model's grid, both box and column processes, such as chemistry, photolysis, radiation, and sedimentation. These discrepancies can be resolved by using consistently Lagrangian methods for the core and (implicitly) for the tracer transport. Here we regard two Lagrangian methods, which divide the atmosphere by mass and present a transformation for these methods to derive a partitioning of the atmosphere in disjunct volumes and masses, which is a necessary pre-requisite to calculate any box or column process.

**Keywords:** Lagrangian modelling, chemistry, transformations

## 1 Introduction

Transport processes are a key aspect in atmospheric modelling. Dispersion modelling, emitter-receptor relations, as well as climate-chemistry modelling rely on accurate transport modelling. Wernli and Davies (1997) used the Lagrangian particle model LAGRANTO, which is driven by data from a numerical weather prediction model to analyse extra-topical cyclones. A large number of particles were evenly distributed in a given Eulerian grid and each trajectory gets a number of properties. Another example, among many others, is given by Stohl et al. (2005), describing the Lagrangian transport model FLEXPART in a similar manner. One option of FLEXPART is to distribute the particles, which all have equal mass, globally or in a given region, according to the atmospheric density. A different approach is applied in the ClaMS-3D model (McKenna et al., 2002a,b; Konopka et al., 2004). Particles are advected and subsequently mixed. The mixing is irreversible and includes dissolving and new creation of particles, which is driven by the wind shear and the resulting potential deformation of air parcels. Two systems of vertical layers are alternating to prevent clustering around the layer center. The particles contain properties like mixing ratios of chemical species, temperature and pressure. The air density is derived from the temperature and pressure and the volume is derived from the (alternating) layer thickness and an area associated to the particle by triangulation of all particles. Thus the actual mass of a chemical species associated to the particle can be derived from its density and volume. Konopka et al. (2004) show that this scheme is mass conserving on a global scale.

Common to these applications is that the simulated properties do not feed back to the dynamics, so-called passive transport studies. For example simulated ozone and water vapour distributions do not feed back to the radiation scheme and influence the atmospheric flow. Stenke et al. (2008) applied the climate model ECHAM4.L39(DLR) with the Lagrangian transport scheme ATTILA for simulating atmospheric water vapour and cloud water, which includes a large feed back to the atmospheric dynamics. They showed that the improved vertical and horizontal water vapour gradients, compared to the standard semi-Lagrangian advection scheme, lead to large changes in the lower stratosphere water vapour concentrations and avoid thereby the large cold bias in that region, common to many climate models. Particles in ATTILA all have the same mass, and transport water vapour mixing ratios. The mixing ratios are mapped to the standard grid of the climate model, where the parameterisations, like cloud formation, rain out, radiation, etc. are computed. Changes in the concentrations are then mapped back to the particles. A similar approach was performed for a chemistry application (Stenke et al., 2009), showing that the simulation of the ozonopause and the location of the ozone hole is bet-

*Corresponding author: Volker Grewe, Deutsches Zentrum für Luft- und Raumfahrt, Institut für Physik der Atmosphäre, Münchener Straße 20, 82234 Weßling, Germany, e-mail: volker.grewe@dlr.de


DOI 10.1127/0941-2948/2014/0552
Gebrüder Borntraeger Science Publishers, Stuttgart, www.borntraeger-cramer.com

ter simulated than using the semi-Lagrangian advection scheme.

All of these simulations have a deficit, which is an inconsistent simulation of the air density distribution between the Lagrangian space and the corresponding Eulerian grid. Fig. 1 sketches this inconsistency: Assume that we have a Lagrangian representation of the concentration of species ($c_L$ in [molecules cm$^{-3}$]), the air density $\rho_L$ (in [kg m$^{-3}$]) and therefore also the volume mixing ratios $vmr_L$ (in [mol mol$^{-1}$]). As soon as local inconsistencies between the Lagrangian and the Eulerian representation of the air density field occur, there is no way to obtain a consistency between the Lagrangian and the Eulerian representation of the concentrations, volume mixing ratios and grid box masses. And hence, as soon as processes are solved in the grid space, e.g. column processes, such as radiation, photolysis, sedimentation and rain (including below-cloud evaporation), inevitable errors occur.

The discrepancy between Eulerian and Lagrangian tracer and mass distributions are shown exemplarily for Radon ($^{222}$Rn) in Fig. 2. The simulation is performed with the chemistry-climate model EMAC (Jöckel et al., 2010). For any arbitrary time step the simulated Radon volume mixing ratios agree between the Eulerian and Lagrangian approach in terms of general structure and absolute values. However, discrepancies can be clearly seen on small scale structures, which mainly arise from deviations in the mass representation (Fig. 2, bottom).

This dilemma can be resolved, by introducing either Lagrangian and hybrid cores for solving the equations of motion, which ensures a consistent representation of air density. Two of these methods, the Finite Mass Method (FMM, Gauger et al., 2000) and the Hamiltonian Particle-Mesh Method (HPM, Frank et al., 2002) are briefly introduced in the following section. However, these methods have been used to simulate (atmospheric) flows, but not yet additional processes, such as atmospheric chemistry. We present transformations (Sec. 3) for either method, which are required to calculate chemical and physical processes on the particles and further show that masses are conserved and densities are consistently described between the different grid representations. Although the transformation is valid for arbitrary processes, we present them exemplarily for chemistry applications.

# 2 Particle methods

In this Section, we summarise two methods to solve the equations of motion, which are based on Lagrangian methods. We follow the nomenclature normally used for these methods. We use the wording mass packets in Sec. 2.1 to suggest that these are fully three dimensional objects, whereas in Sec. 2.2 particles refer to points in the atmosphere.

## 2.1 Finite mass method

The finite mass method was introduced in Gauger et al. (2000); Klingler et al. (2005) and it is based on concepts developed by Yserentant (1997, 1999a,b). Here, we give a short overview (Klingler et al., 2005, see). This gridless Lagrangian method is based on a discretisation of mass, not of space. Mass is subdivided into $N$ small mass packets. Their movement is driven by internal and external forces, and the laws of thermodynamics. Normally, the mass packets overlap. The approximations, which the finite mass method delivers, are smooth functions and not discrete measures.

Each mass packet $i$ has a mass $m_i$ and an internal mass distribution, which is described by a shape function $\psi$ with a normalisation condition and the body coordinate $y$:

$$\int \psi(y)\,dy = 1, \quad \int \psi(y) y\,dy = 0. \tag{2.1}$$

Klingler et al. (2005) used a 3$^{\text{rd}}$ order B-spline as a base function for each space dimension and a tensor product of these base function for $\psi$. The mass packets can move and deform linearly. The points y of the mass packet $i$ move along trajectories:

$$t \;\rightarrow\; q_i(t) + H_i(t)y, \quad \det H_i(t) > 0, \tag{2.2}$$

where $q_i(t)$ is the position of the mass packet center and $H_i(t)$ the deformation matrix. The volume of the mass packet is $V_i(t) = \det H_i(t)$. The prognostic equations for $q_i$ and $H_i$ are derived, based on a classical mechanics approach, by Lagrange functions ($\mathcal{L}$) that is the difference of kinetic and internal energy ($\mathcal{L} = E - V$) (see e.g. Klingler et al., 2005):

$$\frac{d}{dt}\frac{\partial \mathcal{L}}{\partial q_i'} - \frac{\partial \mathcal{L}}{\partial q_i} = 0 \tag{2.3}$$

$$\frac{d}{dt}\frac{\partial \mathcal{L}}{\partial H_i'} - \frac{\partial \mathcal{L}}{\partial H_i} = 0 \tag{2.4}$$

The air density at a location $x$ is the sum of the air density of the overlapping mass packets at that point:

$$\rho(x,t) = \sum_{i=1}^{N} m_i \psi_i(x,t), \text{ with} \tag{2.5}$$

$$\psi_i(x,t) = \frac{\psi\left(H_i(t)^{-1}(x - q_i(t))\right)}{\det H_i(t)}. \tag{2.6}$$

## 2.2 Hamiltonian particle-mesh method

Contrary to the FMM the HPM method utilises a large number of particles. Each carries a mass $m_i$ (computed at the initial time-step, only), but no volume (Tab. 1). The particle mass distribution is used to derive a pressure gradient, which is used in the equations of motion. The HPM method utilises a longitude-latitude grid

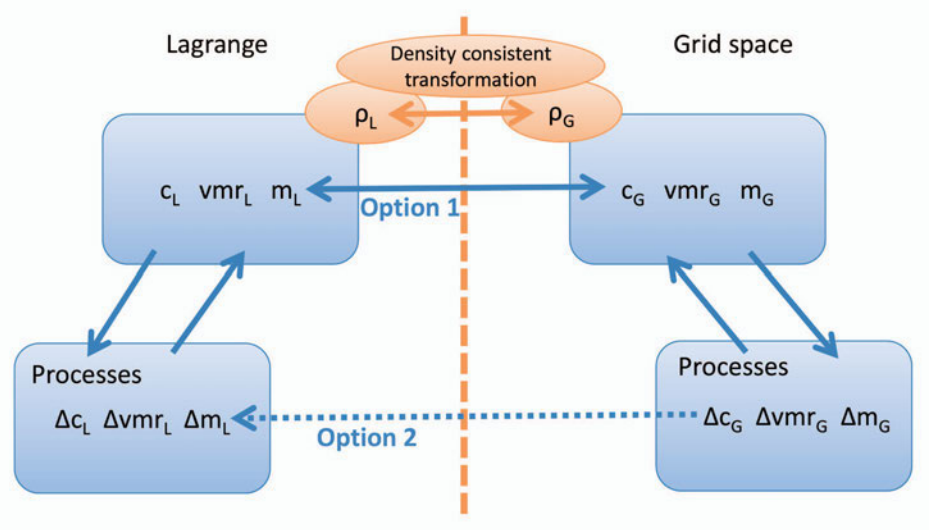


**Figure 1:** Sketch of relations between Lagrangian representation of air density ($\rho_L$), concentrations ($c_L$), volume mixing ratios ($vmr_L$) and masses $m_L$ (left) and the Eulerian grid (right). Processes can be solved in the Lagragian representation or the Eulerian representation. For the Eulerian representation a consistent transformation has to be used to avoid mass inconsistencies (orange), i.e. a pre-requisite is that the densities are equal in the two representations ($\rho_L = \rho_G$). The back transformation of results from the Eulerian process calculations has two options, either changes in the concentration are mapped back to the particles or the new concentrations are mapped back.

**Table 1:** Comparison of the main characteristics of the FMM and HPM method in a typical simulation of the global atmosphere.

| Characteristics | FMM | HPM |
|---|---|---|
| Number of particles | $N$ =100,000 | $N$ =1,000,000 |
| Masses | Each particle may have different, but constant masses, e.g. atmospheric mass divided by $N$ | |
| Volume | Defined by a deformation matrix | No volume |
| Prognostic variable | Center of particle and deformation matrix | Center of particle and pressure gradient from particle mass distribution |
| Auxiliary grid | Quadrature points for each particle | Regular grid |
| Transformation | Reshaping with non-overlapping volumes | Inversion of the smoothing function to attribute parts of the grid volume to particle volume |

with equal grid spacing. The mass distribution on the grid within a model layer is calculated by using a tensor product cubic B-spline $\psi^{mn}(\lambda,\phi)$ of an arbitrary point $x=(\lambda,\phi)$ and the pre-defined auxiliary grid points $(\lambda_m,\phi_n)$:

$$\psi^{mn}(x) = \psi_{cs}\left(\frac{\lambda-\lambda_m}{\Delta\lambda}\right)\psi_{cs}\left(\frac{\phi-\phi_n}{\Delta\phi}\right), \qquad (2.7)$$

where $\psi_{cs}$ is a cubic B-spline. Note that $\psi^{mn}(x)$ differs from zero only for grid points in the neighbourhood of the particle position $x$.

## 3 Transformations for chemistry applications

The calculation of chemical processes requires the concentrations of species (molecules per volume) in a well defined volume. The FMM divides the atmospheric mass in overlapping mass packets and hence the air density and the concentration of a species at a certain point of the atmosphere is defined by a sum of the contributions of all overlapping mass packets. Generally, an individual packet and its mass do not describe the actual air density or concentration at a given point. Therefore a reshaping of the mass packets is necessary for the calculation of chemical processes. This reshaping has to guarantee that mass packets are disjunct and describe the atmospheric mass, volume and concentrations at the given point. Note that we consider a process or operator splitting, i.e. first the equation of motion are solved in a Lagrangian framework and secondly other (e.g. chemical) processes are considered. Sec. 3.1 introduces the reshaping of the mass packets, by defining central masses and volumes for each mass packet, which are subsets of the mass packet (see Fig. 1), so that volumes of these reshaped packets are disjunct (see also Tab. 1).

In contrast, the HPM includes a large number of particles, which represent mass points without volume. Smoothing functions (eq. (2.7)) are used to derive air densities on a grid. In Sec. 3.2 these functions are utilised to derive consistent concentrations.

These two approaches, the FMM and HPM method, describe the calculation of processes, such as chemistry, on the particles. However, for some processes, mainly column processes, such as photolysis, radiation, or sedimentation, it is favourable to introduce a regular grid,

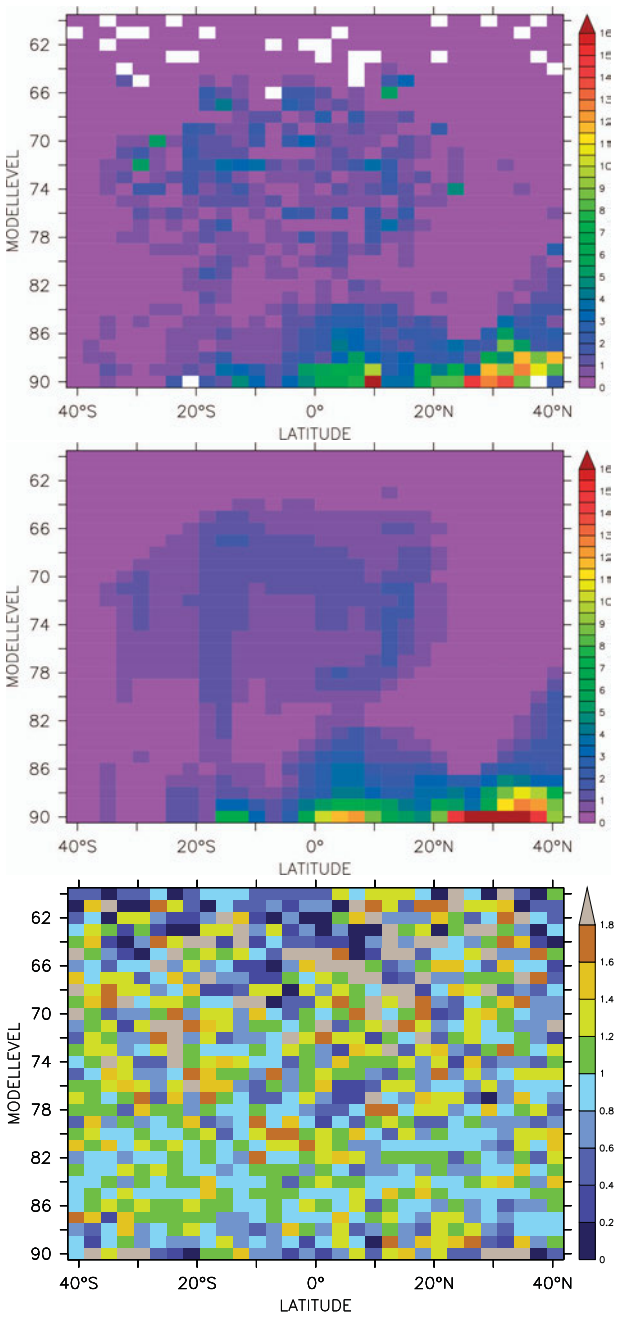


**Figure 2:** Simulated Radon $^{222}$Rn volume mixing rations [mol/mol] at 40° E for December 1st using the Lagrangian transport scheme ATTILA (top) and an Eulerian scheme (mid) in an EMAC simulation (see details in the text). Bottom: Ratio of the air mass distribution in the Lagrangian space mapped on the Eulerian EMAC grid and the mass distribution of the EMAC core. Results are given for model levels, where level 90 is the lowermost level and level 60 roughly 80 hPa.

transfer the information from the Lagrangian space onto this grid and map the calculated change from the grid to the Lagrangian particles in a consistent manner (see also Fig. 1). This is described for FMM and HPM method in Sec. 3.3.

## 3.1 Chemistry in FMM

The mass mixing ratio $c(x)$ (in [kg/kg]) of any species $c$ is defined by

$$c(x) = \rho(x)^{-1} \sum_{i=1}^{N} c_i m_i \psi_i(x), \tag{3.1}$$

where $c_i$ is the mass mixing ratio of the regarded species for the mass packet $i$. (Note that most quantities are time dependent, which is omitted in this section for simplicity reasons.)

We define a degree of overlap ($\kappa$), i.e. the number of mass packets, which contribute information to the point $x$ (see also Fig. 3):

$$\kappa(x) = |\mu(x)| \text{ with} \tag{3.2}$$
$$\mu(x) = \{i | \psi_i(x) > 0\}, \tag{3.3}$$

being the set of mass packet indices contributing to $x$ and $|\cdot|$ the number of elements. We now reshape each volume $V_i$ and mass $m_i$ into non-overlapping central volumes $\hat{V}_i$ and central masses $\hat{m}_i$ for each mass packet $i$, which contain the non-overlapping volume and only parts of the over-lapping volumes:

$$\begin{aligned} \hat{V}_i &= V_i - \int_{\mathcal{V}_i} \left(1 - \frac{1}{\kappa(x)}\right) dx \\ &= \int_{\mathcal{V}_i} \frac{1}{\kappa(x)} dx \text{ with} \\ \mathcal{V}_i &= \{x | \psi_i(x) > 0\}. \end{aligned} \tag{3.4}$$

$\hat{\mathcal{V}}_i$ are arbitrary disjunct sets such that $\hat{\mathcal{V}}_i \subseteq \mathcal{V}_i$ and $\int_{\hat{\mathcal{V}}_i} dx = \hat{V}_i$. Equation (3.4) implicitly defines the central volumes. For example a region which is overlapped by $\kappa(x)$ volumes is split into $\kappa(x)$ equally sized parts. The shapes of these parts are not important to our method.

Similarly, we define the masses $\tilde{m}_i^j$ of the non-overlapping volumes for two overlapping mass packets $i$ and $j$. The part of the mass of mass packet $j$, which contributes to the mass of the central volume $\hat{V}_i$ of mass packet $i$ is $\tilde{m}_i^j$:

$$\begin{aligned} \tilde{m}_i^j &= \begin{cases} \int_{\mathcal{V}_i} \frac{m_j \psi_j(x)}{\kappa(x)} dx & j \neq i \\ m_i - \int_{\mathcal{V}_i} \frac{\kappa(x)-1}{\kappa(x)} m_j \psi_j(x) dx & j = i \end{cases} \\ &= \int_{\mathcal{V}_i} \frac{m_j \psi_j(x)}{\kappa(x)} dx \end{aligned} \tag{3.5}$$

The central mass $\hat{m}_i$, i.e. the mass which corresponds to the volume $\mathcal{V}_i$ is then

$$\hat{m}_i = \sum_j \tilde{m}_i^j \tag{3.6}$$

It can easily be shown (by using eq. (3.4)) that

$$\sum_i \hat{m}_i = \sum_i m_i, \tag{3.7}$$

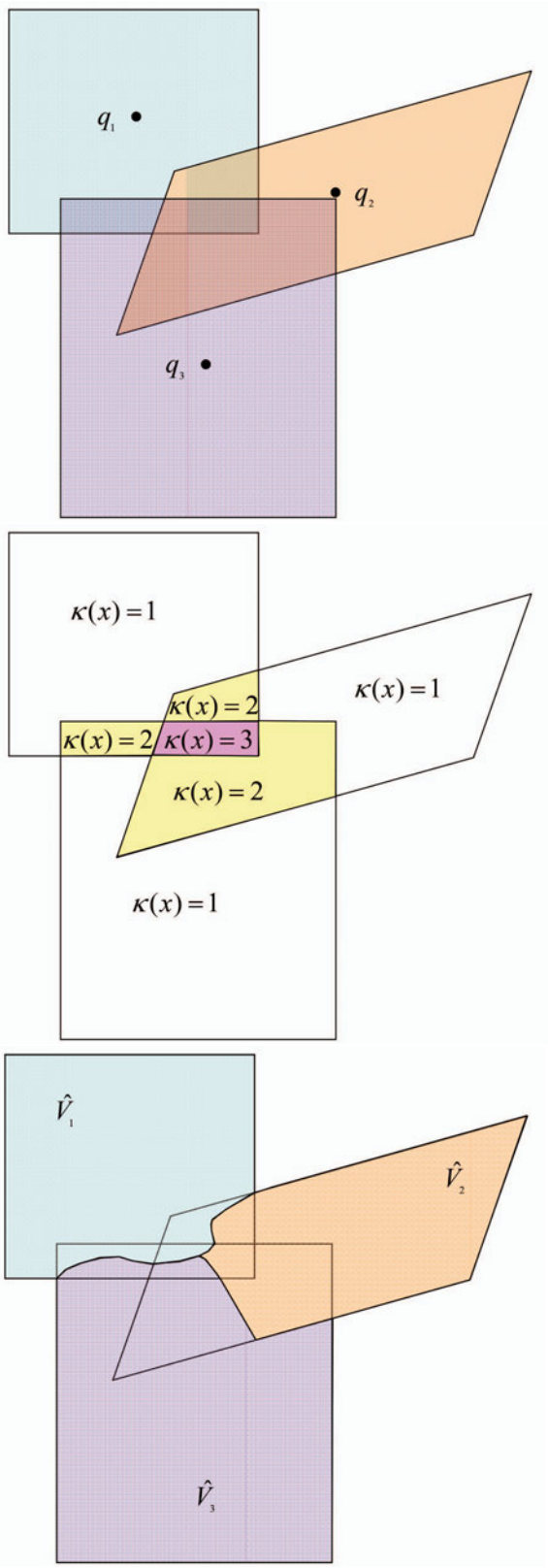


**Figure 3:** Illustration of the reshaping of mass packets for the Finite Mass Method. $q$ is the position of the center of the mass packets, $\kappa$ is the number of overlapping volumes, and $\hat{V}$ the center volumes. The first part shows exemplarily three mass packets which are overlapping. The second part illustrates how the overlapping index $\kappa$ is defined. The third part illustrates the re-shaping of the mass packets to center volumes, which are not overlapping anymore. Note that their shape is arbitrary. (Details see text).

i.e. the mass is disjunctly partitioned to volumes $\hat{V}_i$. The fraction of an individual mass packet $j$ to the central mass of the mass packet $i$ is

$$\hat{\chi}_j^i = \frac{\tilde{m}_i^j}{\hat{m}_i} \text{ with} \tag{3.8}$$

$$\sum_j \hat{\chi}_j^i = 1 \tag{3.9}$$

and the air density of the central volume is

$$\hat{\rho}_i = \frac{\hat{m}_i}{\hat{V}_i}. \tag{3.10}$$

For any chemical species with the mass fraction in the part of the mass packet $j$, which contributes to the center volume $\hat{V}_i$ follows the mass definition (eq. (3.5)):

$$\tilde{c}_i^j = \frac{1}{\tilde{m}_i^j} \int_{\mathcal{V}_i} \frac{m_j \psi_j(x)}{\kappa(x)} dx \tag{3.11}$$

and hence the mean concentration $\hat{c}_i$ in the central volume $\hat{V}_i$ is:

$$\hat{c}_i = \frac{1}{\hat{m}_i} \sum_j \tilde{c}_i^j \tilde{m}_i^j \tag{3.12}$$

This mass packet reshaping is globally mass conserving ($C$ is the atmospheric mass of the regarded species):

$$\begin{aligned} \sum_i \hat{c}_i \hat{m}_i &= \sum_i \sum_j \tilde{c}_i^j \tilde{m}_i^j \\ &= \sum_{i=1}^N \sum_{j=1}^N \int_{\mathcal{V}_i} \frac{c_j m_j \psi_j(x)}{\kappa(x)} dx \\ &\overset{(3.4)}{=} \sum_{i=1}^N \sum_{j=1}^N \int_{\hat{\mathcal{V}}_i} c_j m_j \psi_j(x) dx \\ &= \int_V \sum_{j=1}^N c_j m_j \psi_j(x) dx \\ &= \int_V c(x) \rho(x) dx \\ &= C. \end{aligned} \tag{3.13}$$

Chemical processes are now solved for the central volumes and with the mass mixing ratios $\hat{c}_i$. With the resulting changes $\Delta\hat{c}_i$ the respective changes $\Delta\tilde{c}_i^j$ for the overlapping masses $m_i^j$ are:

$$\Delta\tilde{c}_i^j = \frac{\Delta\hat{c}_i \tilde{m}_i^j}{\hat{m}_i} \tag{3.14}$$

and the changes $\Delta c_i$ for the original mass packets are:

$$\Delta c_i = \sum_{i=1}^N \Delta\hat{c}_i. \tag{3.15}$$

This back transformation from the center volumes to the original mass packets is again mass conserving,

which can be easily shown in analogy to eq. (3.13). Note, this back transformation assumes that the individual overlapping mass packets are contributing to chemical changes with the same ratio as they contribute to the mass. Alternatively, this back transformation can be achieved by calculating this contribution according to the chemical composition via the tagging method (GREWE et al., 2010; GREWE, 2013). This will provide an alternative and probably more consistent definition of $\tilde{c}_i^j$ in eq. (3.11), but it does not affect the calculation in eq. (3.13) and hence the mass conservation.

## 3.2 Chemistry in HPM

The HPM method provides a mapping of the mass distribution from $N$ particles on a grid with gridpoints $\zeta_k$ (see also Sec. 2.2):

$$\rho : (\zeta_k, q_1, \ldots, q_N, m_1, \ldots, m_N) \tag{3.16}$$
$$\longmapsto \rho(\zeta_k, q_1, \ldots, q_N, m_1, \ldots, m_N) \tag{3.17}$$
$$= \sum_i m_i \Psi^i(\zeta_k) V_k^{-1} \tag{3.18}$$
$$=: \rho^k, \tag{3.19}$$

where $\Psi$ is a basis function satisfying the property of partitioning of unity to guarantee mass conservation and $V_k$ the grid volume of $\zeta_k$, i.e.

$$\sum_k \Psi^i(\xi_k) = 1, \text{ and} \tag{3.20}$$
$$\sum_k \rho^k V_k = \sum_i m_i. \tag{3.21}$$

We now need to map the densities $\rho_k$, which are defined on the grid, onto the positions of the particles in a mass conserving manner. This can be achieved by using the already calculated B-splines for partitioning of the grid volume (see below eq. (3.23)). Each particle contributes to the air density of a number of grid points (eq. (3.19)). At the grid point $\zeta_k$ this relative contribution $z_k^i$ is

$$z_k^i = \frac{m_i \Psi^i(\zeta_k)}{\sum_j m_j \Psi^j(\zeta_k)}. \tag{3.22}$$

We now associate a volume $\hat{V}_i$ to particle $i$ by using this relative contribution:

$$\hat{V}_i = \sum_k V_k z_k^i. \tag{3.23}$$

Thereby the masses and volumes are consistently defined for both the grid and the particles, with

$$\sum_i \hat{V}_i = \sum_i \sum_k m_i \frac{\Psi^i(\zeta_k)}{\rho_k} \tag{3.24}$$
$$= \sum_k \rho_k^{-1} \sum_i m_i \Psi^i(\zeta_k) \tag{3.25}$$
$$= \sum_k V_k. \tag{3.26}$$

**Table 2:** Mixing ratios of an arbitrary species at timestep $t_0$ and after a quadratic loss term is calculated ($t_1$). P1 and P2 indicate particle 1 and 2.

| Time | Loss simulated on particles | | | Loss simulated on grid | | |
|---|---|---|---|---|---|---|
| step | P1 | P2 | Mean | Grid Mean | P1 | P2 |
| $t_0$ | 0.10 | 0.9 | 0.5 | 0.5 | 0.1 | 0.9 |
| $t_1$ | 0.09 | 0.09 | 0.09 | 0.25 | 0.175 | 0.675 |

The air density of the particle is simply $\hat{\rho}_i = m_i / \hat{V}_i$, For a given mass of a species $c_i^m$ on the particle $q_i$, the mass mixing ratio and the concentration of this species are simply obtained using the mass and air density of the particle.

## 3.3 Chemistry on a grid

Section 3.1 and 3.2 described how Lagrangian particles have to be treated in the FMM and HPM method for a calculation of chemical processes on the particle. However, there are processes, which require column information, such as sedimentation, radiation, and photolysis. In that case, particle information has to be transferred to a regular grid, the regarded process simulated on that grid and the calculated changes re-transferred to the Lagrangian particles.

The FMM is basically grid free, for numerical integrations, a secondary grid is used, which moves with the particles. Hence, we suggest to introduce a grid in a way, as it is done for the HPM method (see above) and refer to the nomenclature in Sec. 3.2. The concentration on the grid ($c(\zeta_k)$) can be calculated in analogy to the air density calculation ($\rho_k$, eq. (3.19)). We obtain changes of the concentration on the grid caused by the regarded process: $\Delta c(\zeta_k)$. For linear processes, all particles which contribute to the concentration are contributing in the same manner to the concentration change on the particles ($\Delta c_i$), which follows the idea of the volume $\hat{V}_i$ calculation in eq. (3.23):

$$\Delta c_i = \sum_k \Delta c(\zeta_k) z_k^i. \tag{3.27}$$

However, for non-linear processes, this approach is not valid. Tab. 2 gives a simple example for two particles with mixing ratios of 0.1 and 0.9. We take a quadratic (i.e. non-linear) loss process into account, which leads to loss rates of 0.01 and 0.81 respectively. After the calculation of the loss process both particles have a concentration of 0.09. The grid mean (assuming both particles have the same mass and are fully located in the grid volume) is 0.5 and the loss rate 0.25, which leads to a concentration of 0.25 after the process. Linearly, redistributing this loss leads to concentrations of 0.175 and 0.675, respectively. Obviously this grid processing leads to large errors and non-linear processes should be treated on the particles as far as possible.

## 4 Summary and conclusions

A good representation of transport processes in atmosphere-chemistry models is essential for a reliable estimate of emittor-receptor relations, air quality, or climate-chemistry simulations. Lagrangian methods are well suited to resolve tracer transport. The resulting air density distribution, i.e. the air density distribution based on the particle distribution, often differs from the air density distribution of the model's core, which causes inconsistencies and errors whenever tracers have to be transferred from the Lagrangian space to the grid of the model core. This issue can be resolved by using Lagrangian methods, such as the Finite Mass Method or the Hamiltonian Particle Mesh method, in the model's core. These methods haven't been used for atmospheric chemistry applications yet and they are not right away suited to calculate box or column processes in the Lagrangian space. Here, we present transformations, which allow a consistent and disjunct partitioning of the atmosphere in volumes and masses, which can be used to calculate either box and column processes.

For the Finite Mass Method, which divides the atmosphere into overlapping mass packets, we reshape these packets into new non-overlapping packets, which inherit properties from other overlapping packets. These new packets represent an auxiliary grid which is only used for the process calculation, like chemistry, but does not affect the Finite Mass Method itself. The inversion of the reshaping is used to map the changes from any box process onto the original overlapping mass packets.

The Hamiltonian Particle Mesh method employs particles, which have a mass but no volume, and uses smoothing function to derive pressure gradients from the particle distribution for a regular auxiliary grid. This smoothing can be seen as an extension of the particles from a point to a volume with the use of the auxiliary grid and we invert these functions to derive air density and volume for the particles.

These two transformations divide the atmosphere into disjunct boxes on the particles so that additional process simulations, which need well-defined masses and volumes, such as chemistry can be performed. Column processes, however, are more difficult to calculate in the Lagrangian space and it may be necessary to calculate processes not on the particles but on the auxiliary grid and map the calculated changes back to the particles. We showed that this can be done consistently for linear processes, such as transport or sedimentation. However for non-linear processes, we showed that any mapping and smoothing from the particles to the auxiliary grid may impose large errors compared to the calculation on the trajectories. Hence we suggest to calculate all non-linear processes on the particles and only use an auxiliary grid in cases, where a direct calculation is not possible, such as sedimentation, radiation, or photolysis.

## Acknowledgments

This work was funded by the DFG-project LagKern (GR3314-1/2, YS18/3-2, and RE 2433/4-1) in the DFG-SPP Metström. We gratefully acknowledge the DKRZ. The authors thank the internal reviewer Simon Unterstrasser.

## References

Frank, J., G. Gottwald, S. Reich, 2002: The Hamiltonian particle-mesh method. – In: "Meshfree Methods for Partial Differential Equations". M. Griebel, M.A. Schweitzer (Eds.): Lecture Notes in Computational Science and Engineering **26**, 131–142.

Gauger, C., P. Leinen, H. Yserentant, 2000: The finite mass method. – SIAM J. Numer. Anal. **37**, 1768–1799.

Grewe, V., 2013: A generalized tagging method. – Geosc. Mod. Dev. **6**, 247–253.

Grewe, V., E. Tsati, P. Hoor, 2010: On the attribution of contributions of atmospheric trace gases to emissions in atmospheric model applications. – Geosci. Model Dev. **3**, 487–499.

Jöckel, P., A. Kerkweg, A. Pozzer, R. Sander, H. Tost, H. Riede, A. Baumgaertner,S. Gromov, B. Kern, 2010: Development cycle 2 of the Modular Earth Submodel System (MESSy2). – Geosci. Model Dev. **3**, 717–752. DOI:10.5194/gmd-3-717-2010.

Klingler, M., P. Leinen, H. Yserentant, 2005: The finite mass method on domains with boundary. – SIAM J. Sci. Comput. **26**, 1744–1759.

Konopka, P., H.M. Steinhorst, J.U. Grooss, G. Günther, R. Müller, J.W. Elkins, H.J. Jost, E. Richard, U. Schmidt, G. Toon, D. McKenna, 2004: Mixing and ozone loss in the 1999.2000 Arctic vortex: Simulations with the three-dimensional Chemical Lagrangian Model of the Stratosphere (CLaMS). – J. Geophys. Res. **109**, D02315. DOI:10.1029/2003JD003792.

McKenna, D.S., P. Konopka, J.-U. Grooss, G. Günther, R. Müller, R. Spang, D. Offermann, Y. Orsolini, 2002a: A new Chemical Lagrangian Model of the Stratosphere (CLAMS): 1. Formulation of advection and mixing. – J. Geophys. Res. **107**, 4309. DOI:10.1029/2000JD000114.

McKenna, D.S., J.-U. Grooss, G. Günther, P. Konopka, R. Müller, G. Carver, Y. Sasano, 2002b: A new Chemical Lagrangian Model of the Stratosphere (CLAMS): 2. Formulation of chemistry scheme and initialization. – J. Geophys. Res. **107**, 4256. DOI:10.1029/2000JD000113.

Stenke, A., V. Grewe, M. Ponater, 2008: Lagrangian transport of water vapor and cloud water in the ECHAM4 GCM and its impact on the cold bias. – Climate Dynam. **31**, 491–506. DOI:10.1007/s00382-007-0347-5.

Stenke, A., M. Dameris, H. Garny, V. Grewe, 2009: Implications of Lagrangian transport for coupled chemistry-climate simulations. – Atmos. Chem. Phys. **9**, 5489–5500.

Stohl, A., C. Forster, A. Frank, P. Seibert, G. Wotawa, 2005: Technical note: The Lagrangian particle dispersion model FLEXPART version 6.2. – Atmos. Chem. Phys. **5**, 2461–2474. DOI:10.5194/acp-5-2461-2005.

Wernli, H., H.C. Davies, 1997: A Lagrangian-based analysis of extratropical cyclones. I: The method and some applications. – Quart. J. Roy. Meteor. Soc. **123**, 467–4897.

Yserentant, H., 1997: A particle model of compressible fluids. – Numer. Math. **76**, 111–142.

Yserentant, H., 1999a: Particles of variable size. – Numer. Math. **82**, 143–159.

Yserentant, H., 1999b: Entropy generation and shock resolution in the particle model of compressible fluids. – Numer. Math. **82**, 161–177.